SUPPLEMENTARY METHODS

Microfossil Biostratigraphy

Dinoflagellate Cysts - Samples were crushed to chips of several millimeters, and oven-dried (60 ˚C). The samples were then weighed and transferred to 200 ml plastic bottles with screw-on caps. A tablet containing a known amount of *Lycopodium* spores (18,583 ±4.1 % spores per tablet) was added to each sample as a known spike so quantitative abundances could be calculated. Samples were wetted with 10% Agepon wetting detergent, and subsequently 10 % HCl was added. Subsequently, silicates were removed from all samples by adding an overload of unheated 38% HF. Samples were shaken on a shaker table for 2 hours (300 rpm), bottles were filled up with water, and samples settled overnight. Subsequently, bottles were decanted, and 30% HCl was added to remove silica gels. Sample bottles were centrifuged (2000 rpm, 5 minutes), decanted, and filled to halfway with HF. They were then shaken for 2 hrs on a shaker table (300 rpm), filled up with water, and settled overnight. The next day, samples were decanted, and silica gels were removed again by adding an overload of 30% HCl, centrifuging (2000 rpm, 5 minutes), and decanting. From the acid-resistant organic residues, all samples were sieved over a 250 μm nylon sieve to remove large particles. The filtrate was then sieved at 15 μm. For sieving, an ultrasonic bath was used to disintegrate palynodebris. The organic residue was separated from heavier particles (including pyrite and heavy minerals) by placing it into a ceramic bowl in the ultrasonic bath for five minutes so that the heavy particles settled, and the palynofacies remained suspended. The ceramic bowl was subsequently decanted, and the palynofacies assemblages were transferred into a glass vial. Palynofacies residues were centrifuged (2000 rpm, 5 minutes), decanted, and diluted with glycerine water. The residue was transferred to microscope slides, and slides were sealed using nail polish. Two slides were made for each sample. Dinocyst taxonomy follows that cited in Fensome and Williams (2004). Palynological residues and slides are stored in the collection of the Laboratory of Palaeobotany and Palynology, Utrecht University.

Isotope Geochronology

$^{40}Ar/^{39}Ar$ – For our analysis, the basalt sample was crushed and sieved to 250-350 μm, and the phenocrysts were removed via magnetic sorting. The purified groundmass separate was irradiated for 60 hours at the Oregon State University TRIGA-type reactor in the Cadmium-Lined In-Core Irradiation Tube along with the 28.201 Ma Fish Canyon tuff sanidine (FCs) (Kuiper et al., 2008). At the University of Wisconsin Rare Gas Geochronology Laboratory, ~2 mg of groundmass was incrementally heated using a 25 Watt CO2 laser. The experiment consisted of 22 steps; each step included heating for 60 seconds at a

given laser power, followed by an additional 15 minutes for gas cleanup. The gas was cleaned during and after the heating period with two SAES C50 getters. Blanks were analyzed after every two heating steps.

U/Pb LA-ICP-MS – We utilized a laser-beam diameter of 30 µm, firing at a repetition rate of 7 Hz for 15 seconds with an energy fluence of ~6.2 J/cm2 at the sample surface. All isotopes were simultaneously measured in static mode, with masses 238, 232, 208, 207 and 206 monitored in Faraday detectors while 204 and 202 were measured using ion-multipliers in order to allow reliable common-Pb and Hg interference corrections. Inter-element fractionation corrections and U–Th concentrations were calculated by calibration with respect to an in-house Sri Lanka zircon standard with a known age of 563.5 ± 3.2 Ma (Gehrels et al. 2008). Common-Pb corrections were applied by using the mercury-corrected ^{204}Pb intensities of each individual spot, assuming an initial Pb composition following the model of Stacey and Kramers (1975).

U/Pb CA-TIMS – The eleven zircon crystals selected from the LA-ICP-MS results were plucked from the epoxy mount and annealed in quartz beakers in a muffle furnace at 900°C for 60 hours. Individual grains were then transferred to 3 ml Teflon PFA beakers, rinsed twice with 3.5 M HNO_3, and loaded into 300 ml Teflon PFA microcapsules. The microcapsules were placed in a large-capacity Parr vessel, and the crystals were partially dissolved in 120 ml of 29 M HF with a trace of 3.5 M HNO_3 for 10-12 hours at 180°C. The contents of each microcapsule were returned to 3 ml Teflon PFA beakers, the HF removed and the residual grains rinsed in ultrapure H_2O, immersed in 3.5 M HNO_3, ultrasonically cleaned for an hour, and fluxed on a hotplate at 80°C for an hour. The HNO_3 was removed, and the grains were again rinsed in ultrapure H_2O or 3.5M HNO_3, before being reloaded into the same 300 ml Teflon PFA microcapsules (rinsed and fluxed in 6 M HCl during crystal sonication and washing) and spiked with the EARTHTIME mixed ^{233}U-^{235}U-^{205}Pb tracer solution (ET535), which has been calibrated against the EARTHTIME gravimetric standards. These chemically abraded grains were dissolved in Parr vessels in 120 ml of 29 M HF with a trace of 3.5 M HNO_3 at 220°C for 48 hours, dried to fluorides, and then re-dissolved in 6 M HCl at 180°C overnight. U and Pb were separated from the zircon matrix using an HCl-based anion-exchange chromatographic procedure (Krogh, 1973), eluted together and dried with 2 µl of 0.05 N H_3PO_4.

Pb and U were loaded on a single outgassed Re filament in 2 µl of a silica-gel/phosphoric acid mixture (Gerstenberger and Haase, 1997), and U and Pb isotopic measurements were made on a GV Isoprobe-T multicollector thermal ionization mass spectrometer equipped with an ion-counting Daly detector at the Boise State University Isotope Geology Laboratory. Pb isotopes were measured by peak-jumping all isotopes on the Daly detector for 100 to 150 cycles and corrected for 0.18 ± 0.04%/a.m.u. mass fractionation. Transitory isobaric interferences due to high-molecular weight organics, particularly

on ^{204}Pb and ^{207}Pb, disappeared within approximately 30 cycles, while ionization efficiency averaged 104 cps/pg of each Pb isotope. Linearity (to ≥1.4 x 106 cps) and the associated dead time correction of the Daly detector were monitored by repeated analyses of NBS982, and have been constant since installation. Uranium was analyzed as UO^{2+} ions in static Faraday mode on 1011 ohm resistors for 150 to 200 cycles, and corrected for isobaric interference of $^{233}U^{18}O^{16}O$ on $^{235}U^{16}O^{16}O$ with an $^{18}O/^{16}O$ of 0.00205. Ionization efficiency averaged 20 mV/ng of each U isotope. U mass fractionation was corrected using the known $^{233}U/^{235}U$ ratio of the ET535 tracer solution.

$^{206}Pb/^{238}U$ ratios and dates were corrected for initial ^{230}Th disequilibrium using a Th/U[magma] of 3 ± 10%. All common Pb in analyses was attributed to laboratory blank and subtracted based on the measured laboratory Pb isotopic composition and associated uncertainty. U blanks were <0.1 pg. The weighted mean age error includes analytical uncertainties based on counting statistics, mass fractionation correction, spike and blank subtraction, and ^{230}Th disequilibrium correction, and is appropriate when comparing to other $^{206}Pb/^{238}U$ ages obtained with spikes cross-calibrated with the EARTHTIME gravimetric standards. If used in comparison with ages derived from other U-Pb methods or decay schemes (e.g. Ar/Ar, U-Pb LA-ICP-MS), then the uncertainty in the spike U/Pb ratio and the ^{238}U decay constant can be added in quadrature, respectively.

SUPPLEMENT REFERENCES

Fensome, R.A. and Williams, G.L., 2004, The Lentin and Williams Index of Fossil Dinoflagellates: Dallas, American Association of Stratigraphic Palynologists Foundation, Contributions Series, no. 42, 909 p.

Gehrels, G.E., Valencia, V.A., and Ruiz, J., 2008, Enhanced precision, accuracy, efficiency, and spatial resolution of U-Pb ages by laser ablation–multicollector–inductively coupled plasma–mass spectrometry: Geochemistry Geophysics Geosystems, v. 9, p. Q03017.

Gerstenberger, H. and Haase, G., 1997, A highly effective emitter substance for mass spectrometric Pb isotope ratio determinations: Chemical Geology, v. 136, p. 309–312.

Krogh, T.E., 1973, A low-contamination method for hydrothermal decomposition of zircon and extraction of U and Pb for isotopic age determinations: Geochimica et Cosmochimica Acta, v. 37, p. 485–494.

Kuiper, K.F., Deino, A., Hilgen, F.J., Krijgsman, W., Renne, P. R., and Wijbrans, J.R., 2008, Synchronizing rock clocks of Earth history: Science, v. 320, p. 500–504.

Lowrie, W., 1990, Identification of ferromagnetic minerals in a rock by coercivity and unblocking temperature properties: Geophysical Research Letters, v. 17, p. 159–162.

Stacey, J.S. and Kramers, J.D., 1975, Approximation of terrestrial lead isotope evolution by a two-stage model: Earth and Planetary Science Letters, v. 26, p. 207–221.

SUPPLEMENTARY FIGURE CAPTIONS

Figure DR1 – Photographs of sampling locations for (A) PL-1 Tuff, (B) OR-20 Tuff, and (C) OR-21 Tuff. GPS coordinates for these locations can be found in Table DR1.

Figure DR2 – Benthic foraminifer from Sample RG1002 tentatively assigned to *Cribrorotalia*? sp. (1a, 1b and 1c are different views of the same specimen).

Figure DR3 – Nannofossils observed in Sample OR1016. Key nannofossils observed under light microscopy (1000x) include: (A) calcisphere fragments, (B) *Coccolithus*, (C) *Cruciplacolithus primus*, (D) *Prinsius dimorphosus*. SEM photographs (E-F) show *Cyclagelosphaera*, *Zeugrhabdotus sigmoides*, *Biscutum*, all common K/Pg survivors, and the Cretaceous-aged *Staurolithites*.

Figure DR4 – Dinocysts observed in sample OR1016. (1) *Cerodinium debielii*, (2) *Cyclapophysis monmouthensis*, (3) *Glaphyrocysta divaricata*, (4) *Hystrichosphaeridium tubiferum*, (5) *Senoniasphaera inornata*, (6) *Tanyosphaeridium xanthiopyxides*, (7-8) *Trithyrodinium evittii*. Scale bar = 25 micrometers.

Figure DR5 – U/Pb concordia diagram for sample OR-Tuff-2012.1, analyzed in this study from the upper Salamanca Formation, showing results obtained by LA-MC-ICP-MS. Note the wide age distribution and >67 Ma ages, indicating that this sample is dominated by Mesozoic detrital zircons. See text for details.

Figure DR6 – (A) Acquisition of isothermal remanent magnetization (IRM) for three samples from the Salamanca Formation, showing rapid increase in magnetization intensity reaching saturation near 0.2T suggesting the dominance of a low coercivity mineral. (B-D) Thermal demagnetization of 3-axis IRM (Lowrie, 1990) for each sample, showing unblocking of the soft IRM component around 580°C, indicating magnetite as the dominant carrier of remanent magnetization in these samples.

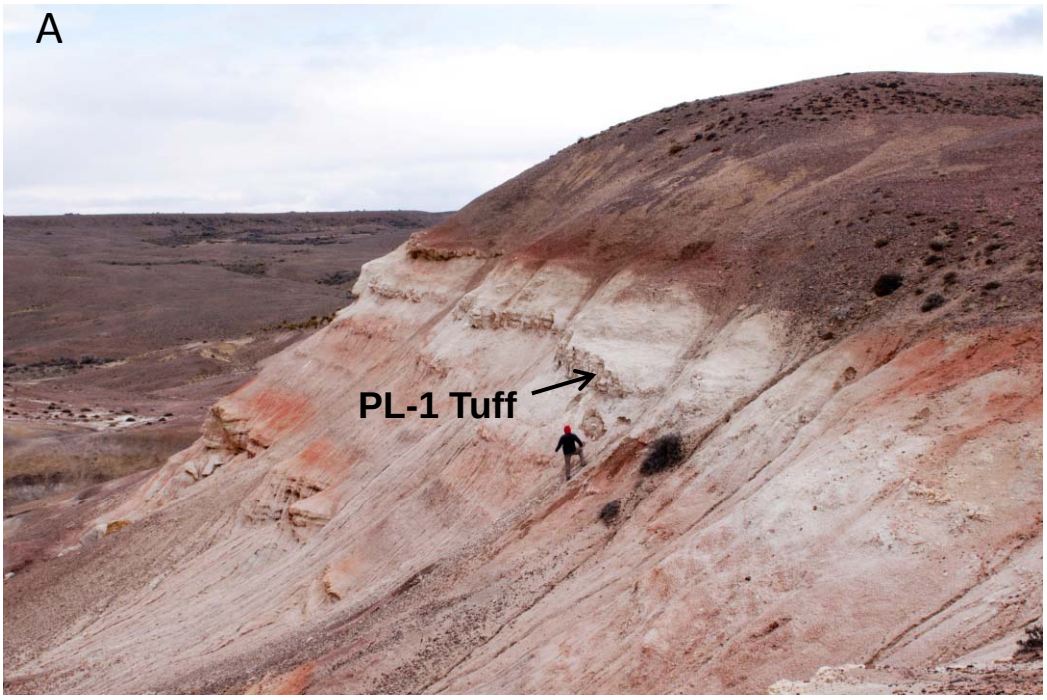

Figure DR1

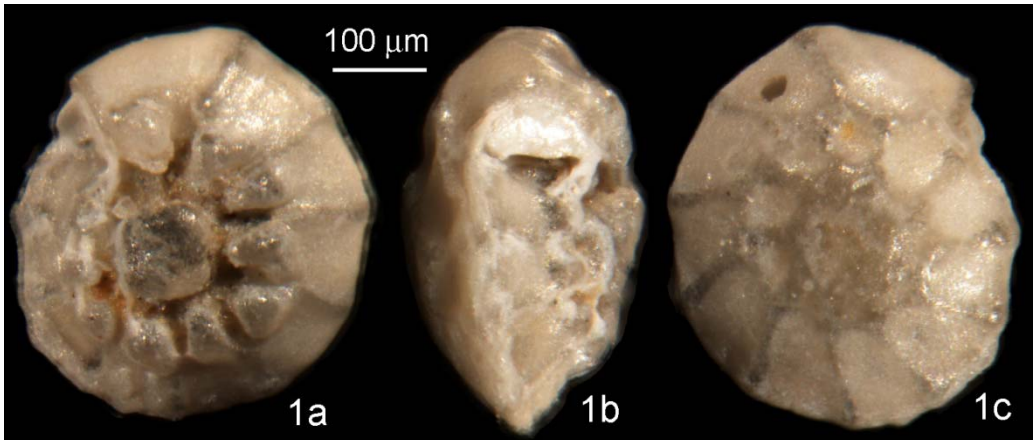

Figure DR2

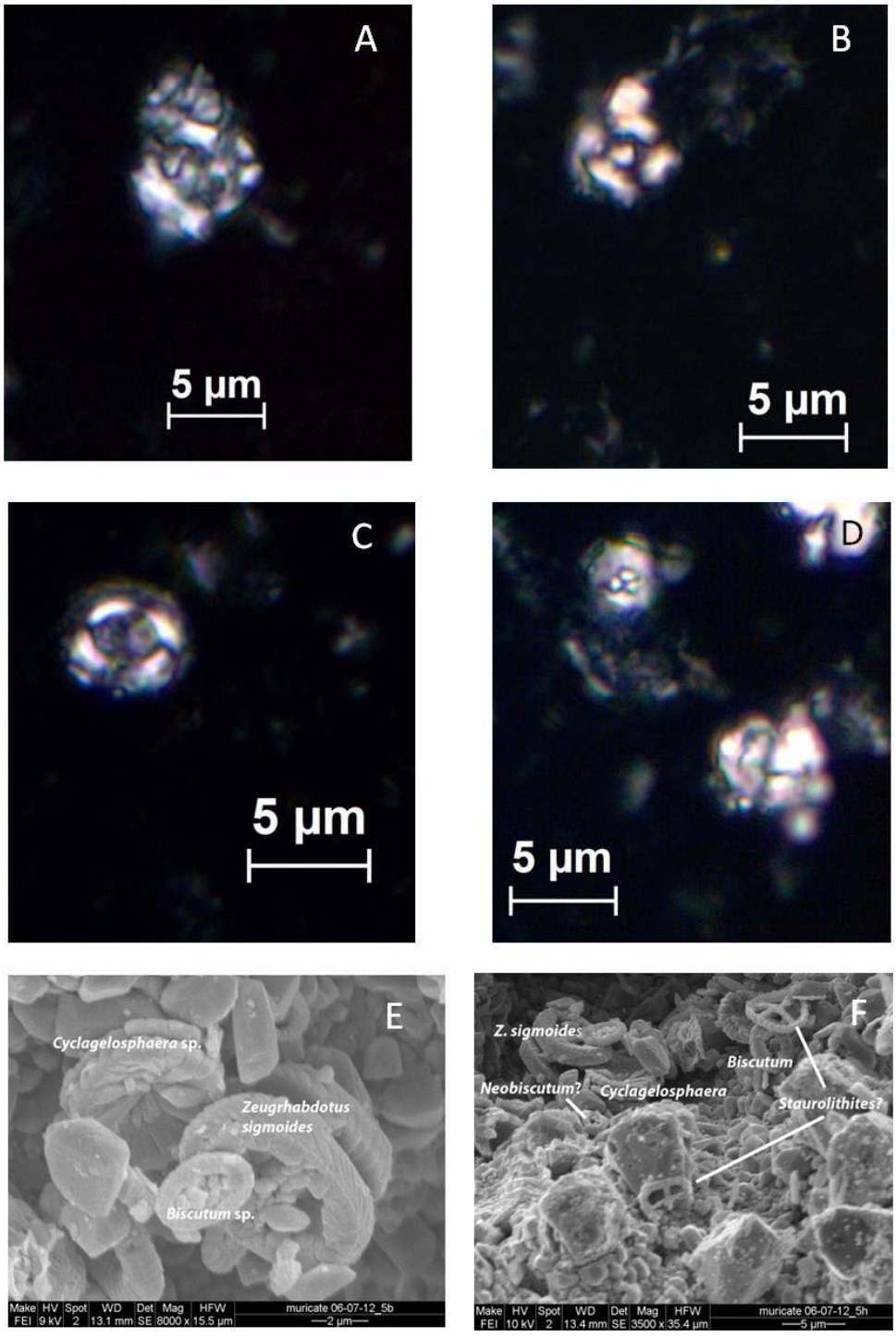
A
5 µm
B
5 µm
C
5 µm
D
5 µm
E
Cyclagelosphaera sp.
Zeugrhabdotus sigmoides
Biscutum sp.
Make HV Spot WD Det Mag HFW muricate 06-07-12_5b
FEI 9 kV 2 13.1 mm SE 8000 x 15.5 µm —2 µm—
F
Z. sigmoides
Biscutum
Neobiscutum?
Cyclagelosphaera
Staurolithites?
Make HV Spot WD Det Mag HFW muricate 06-07-12_5h
FEI 10 kV 2 13.4 mm SE 3500 x 35.4 µm —5 µm—

Figure DR3

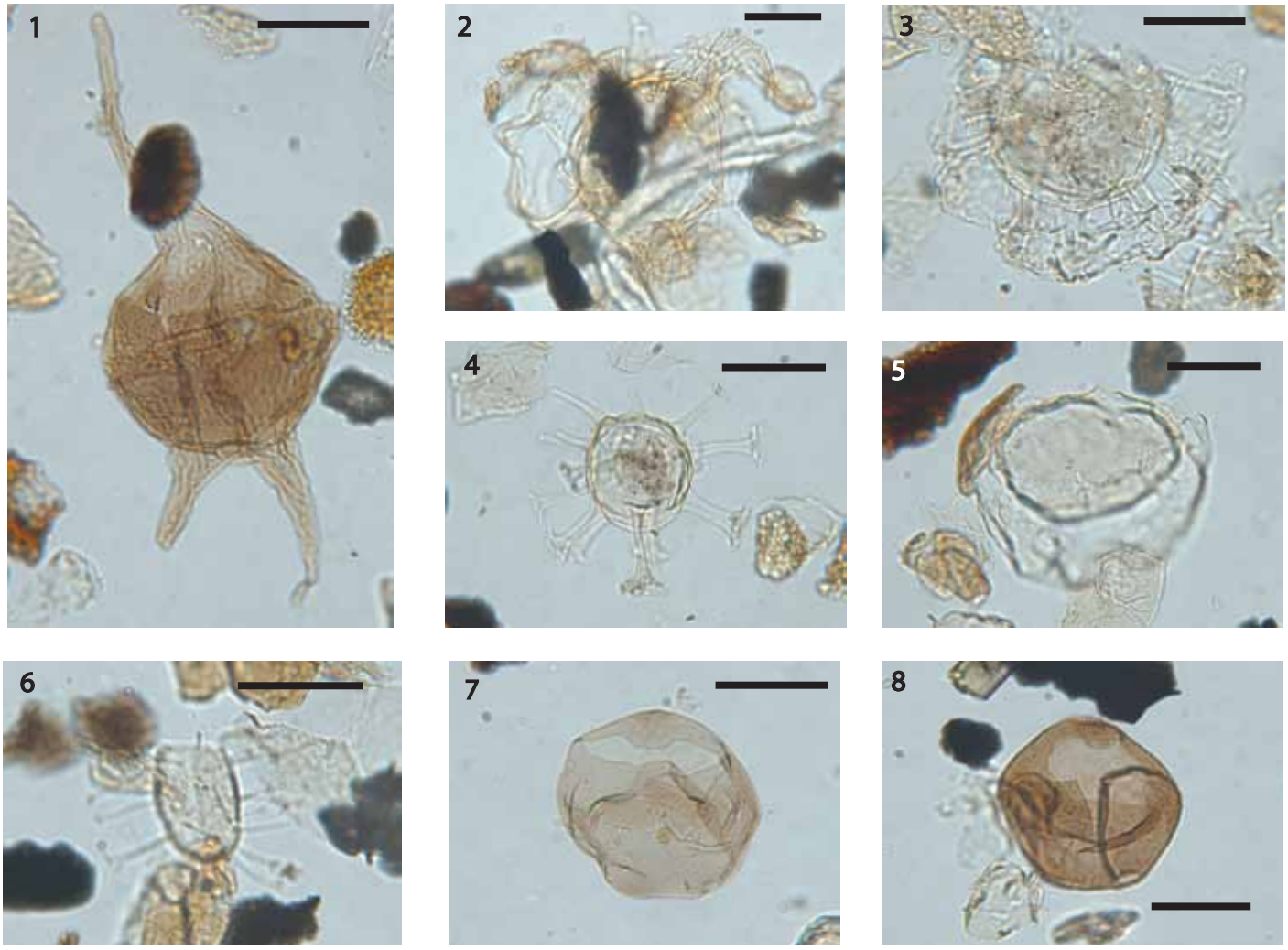

Figure DR4

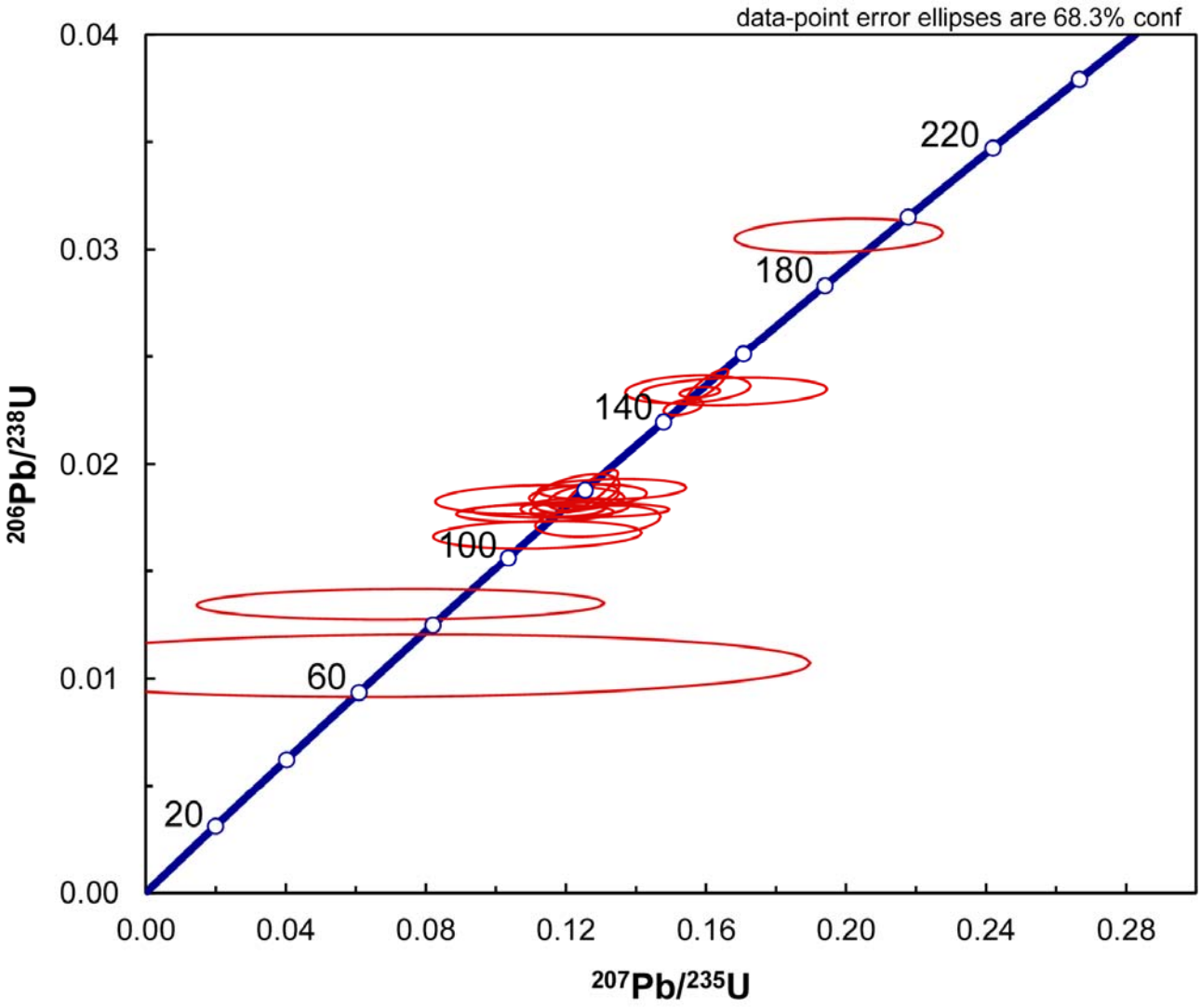
data-point error ellipses are 68.3% conf
0.04
0.03
0.02
0.01
0.00
206Pb/238U
0.00
0.04
0.08
0.12
0.16
0.20
0.24
0.28
207Pb/235U
220
180
140
100
60
20

Figure DR5

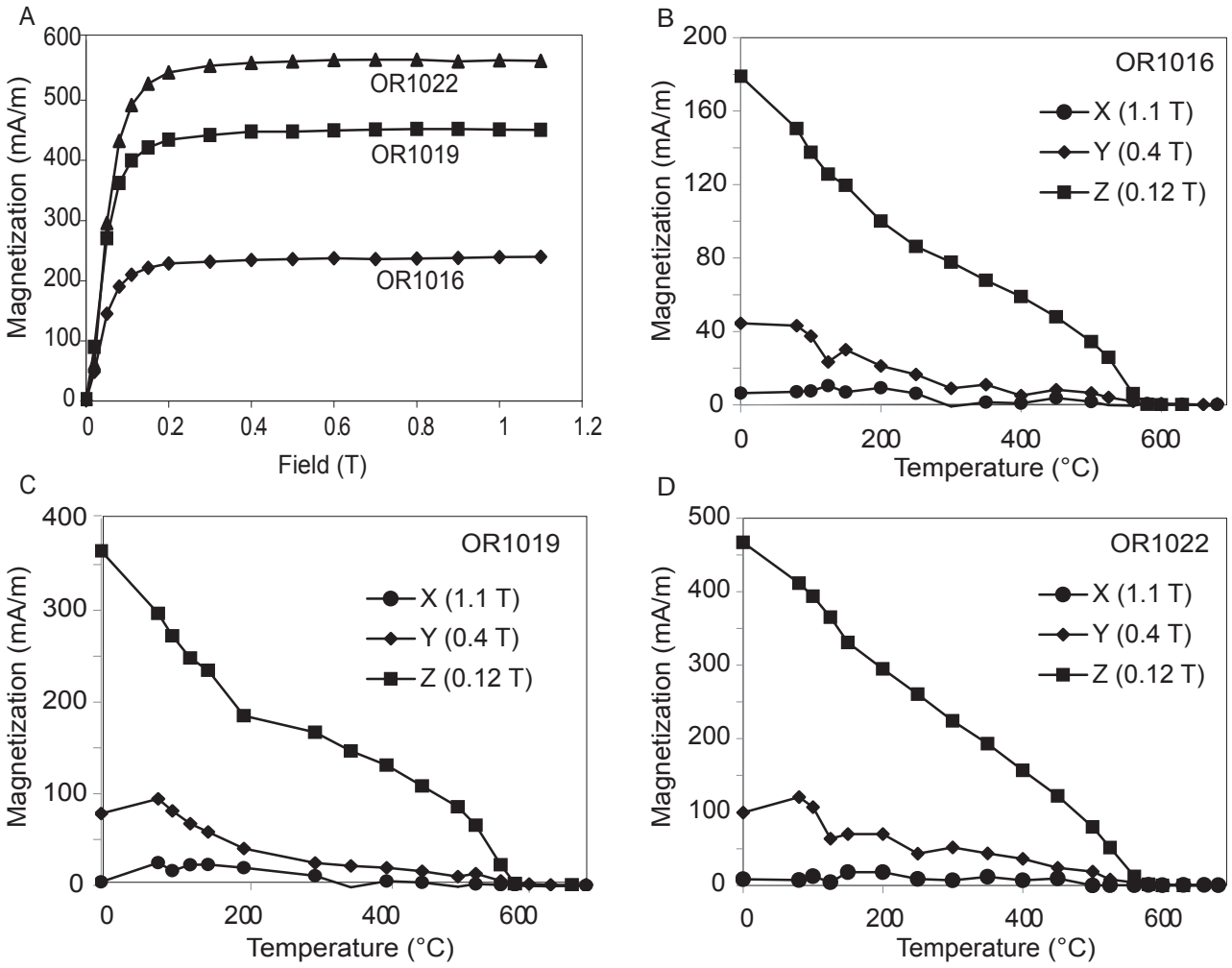
A
Magnetization (mA/m)
Field (T)
OR1022
OR1019
OR1016
B
OR1016
X (1.1 T)
Y (0.4 T)
Z (0.12 T)
Temperature (°C)
C
OR1019
D
OR1022

Figure DR6

Table DR1 - Geographic and stratigraphic location of isotopically dated tuff beds in this study

Sample	Method	GPS Lat (WGS84)	GPS Long (WGS84)	Section	Formation	Local Strat Level (m)	Composite Strat Level (m)
PL-1	U/Pb LA-ICP-MS & TIMS	S45.92137	W69.20368	Palacio de los Loros (b)	Peñas Coloradas	27.5	49.3
OR-20	U/Pb LA-ICP-MS	S45.83431	W69.05163	Cerro Colorado	Peñas Coloradas	28.9	61.5
OR-21	U/Pb LA-ICP-MS	S45.83506	W69.05411	Cerro Colorado	Peñas Coloradas	30.9	63.5
OR-Tuff-2012.1	U/Pb LA-ICP-MS	S45.83244	W69.04725	Cerro Colorado	Salamanca	-3.5	29.1
LF1007	$^{40}Ar/^{39}Ar$	S45.61917	W68.51739	N/A	Basalt between Bajo Barreal & Salamanca	N/A	~ 0

Table DR2 - Stratigraphic, geographic and paleomagnetic data for sample sites in this study

Site	GPS Lat (WGS84)	GPS Long (WGS84)	Section	Formation	Local Strat Level (m)	Composite Strat Level (m)	Strike	Dip	N	Dec_{geo}	Inc_{geo}	α_{95}	R	K	VGP_{long}	VGP_{Lat}	Notes
LF1001	S45.6902451	W068.6163569	Las Flores II	Peñas Coloradas	16.3	N/A	0	0	3	309.7	-47.5	17.8	2.96	49.22	207	47.3	LF-1 Leaf Fossil Site
LF1002	S45.6916560	W068.6190284	Las Flores II	Peñas Coloradas	22.2	N/A	0	0	3	52.3	-61.5	8.3	2.99	224.28	36	53	
LF1003	S45.6271757	W068.4624518	Las Angostura	Bajo Barreal Fm	N/A	N/A	0	0	3	353.2	-61	18	2.96	47.79	235.2	83.9	
OR1001	S45.8084983	W069.0622527	Dromedary Hill	Baja Barreal Fm	-23.2	-23.2	213	3									
OR1002	S45.8085520	W069.0622152	Dromedary Hill	Baja Barreal Fm	-20.2	-20.2	213	3									
OR1003	S45.8086325	W069.0622259	Dromedary Hill	Baja Barreal Fm	-18.4	-18.4	213	3									
OR1004	S45.8087397	W069.0622044	Dromedary Hill	Baja Barreal Fm	-16.2	-16.2	213	3									
OR1005	S45.8087505	W069.0622688	Dromedary Hill	Bajo Barreal Fm	-13.9	-13.9	213	3	3	253.8	68.8	56.5	2.66	5.83	237	-43.3	
OR1006	S45.8088578	W069.0623493	Dromedary Hill	Bajo Barreal Fm	-11.8	-11.8	213	3	3	156.6	49	54.6	2.68	6.17	53.9	-65.8	
OR1007	S45.8089275	W069.0623600	Dromedary Hill	Baja Barreal Fm	-10.2	-10.2	213	3									
OR1008	S45.8090187	W069.0623815	Dromedary Hill	Baja Barreal Fm	-7.3	-7.3	213	3									
OR1009	S45.8091153	W069.0623707	Dromedary Hill	Bajo Barreal Fm	-5.6	-5.6	213	3	3	347.6	-37	38.2	2.83	11.48	264.8	62.9	
OR1010	S45.8094425	W069.0625424	Dromedary Hill	Bajo Barreal Fm	-3.3	-3.3	213	3	3	298.9	-35.4	42.3	2.79	9.55	207.4	33.9	
OR1011	S45.8095498	W069.0625478	Dromedary Hill	Bajo Barreal Fm	-2.1	-2.1	213	3	3	358.7	-49.7	7.4	2.99	276.89	286.7	74.7	
OR1012	S45.8086445	W69.06288055	Dromedary Hill	Salamanca	-0.1	-0.1	213	3									
OR1013	S45.8101774	W069.0633363	Dromedary Hill	Salamanca	0.2	0.2	213	3									
OR1014	S45.8089500	W69.06286667	Dromedary Hill	Salamanca	2.5	2.5	213	3									
OR1015	S45.8100433	W069.0634007	Dromedary Hill	Salamanca	3.3	3.3	213	3									
OR1016	S45.8100379	W069.0633953	Dromedary Hill	Salamanca	5.1	5.1	213	3	3	0.1	-56	22.1	2.94	32.26	291.4	80.7	
OR1017	S45.8098716	W069.0634114	Dromedary Hill	Salamanca	7.1	7.1	213	3	3	349.9	-53	19.9	2.95	39.26	255.2	75.5	
OR1018	S45.8094264	W069.0633363	Dromedary Hill	Salamanca	9.4	9.4	213	3									
OR1019	S45.8093942	W069.0634651	Dromedary Hill	Salamanca	13.0	13.0	213	3									
OR1020	S45.8096410	W069.0634597	Dromedary Hill	Salamanca	31.3	31.3	213	3	3	353.5	-72.5	13.2	2.98	88.3	127	77.4	
OR1021	S45.8096463	W069.0634865	Dromedary Hill	Salamanca	32.4	32.4	213	3	3	350.9	-67.2	15.4	2.97	65.43	163.5	82.6	
OR1022	S45.8096463	W069.0634865	Dromedary Hill	Peñas Coloradas (trans.)	32.6	32.6	213	3	3	347.2	-59.8	20.1	2.95	38.52	225.3	79.4	BNI
OR1023	S45.8270217	W069.0628911	Cerro Colorado	Salamanca	-8.3	24.3	213	3	3	4.6	-64.3	17.8	2.96	49.08	27.4	86.8	OR1 Leaf Fossil Site
OR1024	S45.8276386	W069.0627355	Cerro Colorado	Salamanca	-2.9	29.7	213	3	3	355.5	-69.1	3.3	3	1392.38	132.6	82.6	
OR1025	S45.8276815	W069.0627194	Cerro Colorado	Peñas Coloradas (trans.)	0.0	32.6	213	3	3	2.5	-56.7	21.8	2.94	32.9	304.1	81.2	BNI
OR1026	S45.8276976	W069.0629501	Cerro Colorado	Peñas Coloradas (trans.)	1.1	33.7	213	3	3	14.5	-69.3	15.2	2.97	67.07	63.2	78.2	BNI
OR1027	S45.8277083	W069.0630145	Cerro Colorado	Peñas Coloradas (trans.)	2.7	35.3	213	3	3	3.8	-67.5	12.9	2.98	91.9	83.1	84.8	
OR1028	S45.8273811	W069.0633095	Cerro Colorado	Peñas Coloradas	3.5	36.1	213	3	3	322.8	-54	12.8	2.98	93.39	209.6	59.8	
OR1029	S45.8274669	W069.0637387	Cerro Colorado	Peñas Coloradas	19.9	52.5	213	3	3	200.1	37.6	13.2	2.98	88.28	151.2	-60.3	
OR1030	S45.8275313	W069.0638191	Cerro Colorado	Peñas Coloradas	25.4	58.0	213	3	3	172.5	46	12.6	2.98	96.5	90.5	-70.6	
OR1031	S45.8275957	W069.0638299	Cerro Colorado	Peñas Coloradas	27.9	60.5	213	3	3	162.7	73.6	25.9	2.92	23.78	321.7	-72.9	
OR1032	S45.8273918	W069.0641034	Cerro Colorado	Las Flores	31.3	63.9	213	3	3	356.1	-55.8	4.4	3	778.56	272.4	80.1	
OR1033	S45.8275581	W069.0637655	Cerro Colorado	Peñas Coloradas (trans.)	30.9	63.5	213	3	3	178.5	52.2	27.5	2.91	21.11	105.4	-76.9	
OR1034	S45.8296556	W069.0661312	Cerro Colorado	Las Flores	37.6	70.2	213	3	3	54.4	-51.6	25.4	2.92	24.65	22.5	46.5	
OR1035	S45.8298112	W069.0666462	Cerro Colorado	Las Flores	49.2	81.8	213	3	3	316.2	-65.1	50	2.72	7.14	182.3	60.2	
OR1036	S45.8300848	W069.0669627	Cerro Colorado	Las Flores	56.7	89.3	213	3	3	283.3	-67.4	29.9	2.89	18.01	166.3	40.8	
PL1001	S45.9113879	W069.2097903	Palacio de los Loros (a)	Bajo Barreal Fm	-0.5	-0.5	163	6	3	9.5	-28.6	38.3	2.82	11.4	308.4	58.3	
PL1002	S45.9116472	W069.2102361	Palacio de los Loros (a)	Salamanca	1.4	1.4	163	6									
PL1003	S45.9116917	W069.2102056	Palacio de los Loros (a)	Salamanca	4.1	4.1	163	6									
PL1004	S45.9122837	W069.2107881	Palacio de los Loros (a)	Salamanca	5.3	5.3	163	6	3	8.9	-78.4	27.8	2.9	20.73	101.9	67.7	
PL1005	S45.9121604	W069.2110349	Palacio de los Loros (a)	Salamanca	6.7	6.7	163	6	3	26.4	-45.2	36.8	2.84	12.28	347.4	61.6	
PL1006	S45.9118868	W069.2123813	Palacio de los Loros (a)	Salamanca	11.2	11.2	163	6	3	350.8	-60.4	51.8	2.7	6.73	231.9	81.9	
PL1007	S45.9112699	W069.2123760	Palacio de los Loros (a)	Salamanca	16.0	16.0	163	6	3	336.7	-68	6.2	2.99	390.45	173.8	73.8	PL-1 Leaf Fossil Site
PL1008	S45.9111894	W069.2123974	Palacio de los Loros (a)	Salamanca	19.1	19.1	163	6	3	354.3	-66.8	12.6	2.98	96.15	156.5	84.8	
PL1010	S45.9117151	W069.2139316	Palacio de los Loros (a)	Salamanca	30.1	30.1	163	6	3	349.3	-53.6	20.6	2.95	36.98	252.3	75.7	PL-2 Leaf Fossil Site
PL1011	S45.9116990	W069.2139209	Palacio de los Loros (a)	Salamanca	30.4	30.4	163	6	3	357.8	-64.7	27	2.91	21.94	175.4	88.3	
PL1012	S45.9116400	W069.2139156	Palacio de los Loros (a)	Peñas Coloradas (trans.)	31.0	31.0	163	6	3	12.8	-74.1	11.8	2.98	109.36	87.7	73.7	
PL1013	S45.9114952	W069.2136634	Palacio de los Loros (a)	Peñas Coloradas (trans.)	32.0	32.0	163	6	3	13.4	-63.7	28.7	2.9	19.48	22.1	80.6	BNI
PL1014	S45.9113181	W069.2135937	Palacio de los Loros (a)	Peñas Coloradas (trans.)	32.9	32.9	163	6	3	337.1	-60.9	19.5	2.95	40.96	206.2	73.1	BNI
PL1015	S45.9113664	W069.2134113	Palacio de los Loros (a)	Peñas Coloradas (trans.)	34.1	34.1	163	4	3	347	-71.6	17	2.96	53.46	143.8	76.8	BNI
PL1016	S45.9141613	W069.2167748	Palacio de los Loros (b)	Peñas Coloradas (trans.)	13.2	35.0	163	4	3	345.6	-69.6	23.1	2.93	29.59	156.8	78.1	
PL1017	S45.9141452	W069.2168284	Palacio de los Loros (b)	Peñas Coloradas (trans.)	14.2	36.0	163	4	3	325.4	-57.6	12.9	2.98	91.91	205.1	63.4	
PL1018	S45.9141774	W069.2171342	Palacio de los Loros (b)	Peñas Coloradas (trans.)	15.7	37.5	163	4	3	342.1	-50.7	42.6	2.79	9.43	240.9	70	
PL1019	S45.9140594	W069.2178530	Palacio de los Loros (b)	Peñas Coloradas	20.8	42.6	163	4	3	154.9	57.1	2.3	3	2850.95	35.7	-69.7	
PL1020	S45.9140218	W069.2179442	Palacio de los Loros (b)	Peñas Coloradas	24.3	46.1	163	4	3	160.1	61.2	18.6	2.96	45.07	27.9	-75.3	
PL1021	S45.9140594	W069.2181642	Palacio de los Loros (b)	Penas Coloradas	27.9	49.7	163	4									
RG1001	S45.5463124	W068.2432134	Rancho Grande	Salamanca	2.5	N/A	0	0									
RG1002	S45.5467469	W068.2437820	Rancho Grande	Salamanca	10.5	N/A	0	0									
RG1003	S45.5468220	W068.2437176	Rancho Grande	Salamanca	17.5	N/A	0	0									

Note: GPS Lat/Lon are relative to WGS 1985 datum. Strike/Dip are for bedding orientation. Dec_{geo} and Inc_{geo} are declination and inclination of Characteristic Remanent Magnetization in geographic coordinates. A_{95} is 95% cone of confidence. R is length of resultant vector. K is value of precision parameter. VGP lat/lon are latitude and longitude of virtual geomagnetic pole.

Sample sites with no paleomagnetic data did not pass the Watson test for randomness or were only sampled for micropaleontology

Table DR3 - Complete $^{40}Ar/^{39}Ar$ results for basalt sample LF1007.

N	Laser Power	^{40}Ar	^{40}Ar	$\pm 1\sigma_{40}$	^{39}Ar	$\pm 1\sigma_{39}$	^{38}Ar	$\pm 1\sigma_{38}$	^{37}Ar	$\pm 1\sigma_{37}$	^{36}Ar	$\pm 1\sigma_{36}$	$\%^{40}Ar^*$	$^{40}Ar^*/^{39}Ar_K$	$\pm 1\sigma$	Age	$\pm 2\sigma$	K/Ca
	(%)	(moles)	(Volts)	(Volts)	(Volts)	(Volts)	(Volts)	(Volts)	(Volts)	(Volts)	(Volts)	(Volts)				(Ma)	(Ma)	
1	3.2	1.3163E-14	2.23032	0.00375	0.00601	0.00006	0.00155	0.00004	0.01661	0.00022	0.00752	0.00002	0.39	1.45617	1.35824	40.44	± 74.62	0.155
2	4.2	1.1264E-14	1.90852	0.00373	0.00830	0.00006	0.00140	0.00005	0.01796	0.00023	0.00642	0.00002	0.63	1.45514	0.95243	40.42	± 52.33	0.198
3	4.7	1.0305E-14	1.74610	0.00107	0.01124	0.00005	0.00129	0.00004	0.01928	0.00027	0.00585	0.00002	1.07	1.66720	0.55922	46.23	± 30.63	0.250
4	5.2	9.9024E-15	1.67781	0.00081	0.01652	0.00007	0.00118	0.00004	0.02241	0.00033	0.00560	0.00002	1.53	1.55538	0.32277	43.17	± 17.71	0.317
5	5.7	1.0936E-14	1.85285	0.00072	0.02372	0.00008	0.00144	0.00002	0.02815	0.00034	0.00614	0.00003	2.21	1.72855	0.34192	47.91	± 18.71	0.362
6	6.2	1.1206E-14	1.89860	0.00077	0.03300	0.00008	0.00157	0.00005	0.03484	0.00044	0.00617	0.00002	4.09	2.35595	0.21554	64.99	± 11.68	0.407
7	6.7	1.2395E-14	2.10018	0.00097	0.04782	0.00008	0.00189	0.00006	0.04139	0.00050	0.00673	0.00002	5.45	2.39320	0.15295	66.00	± 8.29	0.496
8	7.2	1.3325E-14	2.25766	0.00125	0.06223	0.00012	0.00208	0.00007	0.05227	0.00065	0.00717	0.00003	6.34	2.30119	0.12729	63.51	± 6.91	0.512
9	7.7	1.2739E-14	2.15849	0.00112	0.06903	0.00018	0.00207	0.00005	0.05596	0.00062	0.00677	0.00002	7.54	2.35781	0.10700	65.04	± 5.80	0.530
10	8.2	1.0348E-14	1.75335	0.00082	0.08563	0.00015	0.00199	0.00005	0.06901	0.00077	0.00525	0.00002	11.82	2.42161	0.07624	66.77	± 4.13	0.533
11	8.7	9.8432E-15	1.66777	0.00106	0.08668	0.00014	0.00196	0.00006	0.07140	0.00079	0.00496	0.00002	12.41	2.38923	0.07355	65.90	± 3.99	0.522
12	9.4	9.2593E-15	1.56884	0.00084	0.09705	0.00017	0.00192	0.00005	0.08173	0.00096	0.00453	0.00002	15.07	2.43786	0.05362	67.21	± 2.90	0.510
13	10.5	1.0504E-14	1.77982	0.00093	0.13135	0.00016	0.00248	0.00006	0.12181	0.00129	0.00498	0.00002	17.92	2.42961	0.04333	66.99	± 2.35	0.463
14	11.5	1.0513E-14	1.78125	0.00095	0.15140	0.00022	0.00274	0.00005	0.15084	0.00159	0.00485	0.00002	20.26	2.38533	0.04571	65.79	± 2.48	0.431
15	12.5	8.9922E-15	1.52359	0.00093	0.14833	0.00018	0.00250	0.00004	0.19398	0.00202	0.00399	0.00002	23.53	2.41854	0.03666	66.69	± 1.99	0.329
16	13.5	8.9217E-15	1.51163	0.00087	0.14704	0.00022	0.00253	0.00007	0.21129	0.00224	0.00398	0.00002	23.19	2.38668	0.03410	65.83	± 1.85	0.299
17	14.5	9.8108E-15	1.66229	0.00084	0.16273	0.00022	0.00272	0.00005	0.23082	0.00247	0.00436	0.00002	23.55	2.40828	0.03568	66.41	± 1.93	0.303
18	15.5	1.0787E-14	1.82771	0.00064	0.21472	0.00021	0.00338	0.00002	0.30784	0.00322	0.00451	0.00002	28.40	2.41956	0.02684	66.72	± 1.45	0.300
19	16.5	1.4161E-14	2.39935	0.00080	0.34074	0.00027	0.00508	0.00004	0.46212	0.00484	0.00544	0.00002	34.51	2.43223	0.01928	67.06	± 1.04	0.317
20	17.5	2.3194E-14	3.92993	0.00147	0.80016	0.00053	0.01097	0.00004	1.84266	0.01898	0.00719	0.00002	49.57	2.43829	0.00891	67.22	± 0.48	0.186
21	18.1	1.5544E-15	0.26338	0.00029	0.03842	0.00009	0.00056	0.00003	0.45113	0.00467	0.00070	0.00001	34.50	2.38356	0.06605	65.74	± 3.58	0.036
22	20.0	1.7821E-15	0.30195	0.00029	0.03547	0.00014	0.00059	0.00004	0.39949	0.00419	0.00085	0.00001	27.36	2.34686	0.07026	64.75	± 3.81	0.038

Note: Weighted mean for 17 of 22 (steps 1-5 excluded) = 66.95 ± 0.37 Ma; Ages calculated relative to 28.201 Ma for the Fish Canyon sanidine (Kuiper et al., 2008) using decay constants of Min et al. (2000);
Atmospheric ($^{40}Ar/^{36}Ar$) ratio = 295.5 (Steiger & Jäger,1977); J-value: 0.0153417 ± 0.000077 (1σ); D/amu: 1.006246 ± 0.000402 (1σ); MSWD = 0.49

Table DR4. U-Pb geochronologic analyses for zircons from Salamanca and Peñas Coloradas tuffs.

				Isotope ratios									Apparent ages (Ma)					
Analysis	U (ppm)	206Pb 204Pb	U/Th	206Pb* 207Pb*	± (%)	207Pb* 235U*	± (%)	206Pb* 238U	± (%)	error corr.	206Pb* 238U*	± (Ma)	207Pb* 235U	± (Ma)	206Pb* 207Pb*	± (Ma)	Best age (Ma)	± (Ma)
PL1TUFF-1	87	4123	1.1	30.0354	96.2	0.0448	96.3	0.0098	5.2	0.05	62.6	3.2	44.5	41.9	-849.8	0.0	62.6	3.2
PL1TUFF-3	450	18010	0.7	21.2488	8.4	0.0619	8.6	0.0095	1.9	0.22	61.2	1.1	61.0	5.1	52.4	201.6	61.2	1.1
PL1TUFF-4	157	6022	0.9	19.6602	20.2	0.0661	20.6	0.0094	3.7	0.18	60.5	2.2	65.0	12.9	234.7	470.9	60.5	2.2
PL1TUFF-5	406	1843	0.9	20.2099	12.0	0.0650	12.3	0.0095	2.5	0.20	61.1	1.5	63.9	7.6	170.6	282.0	61.1	1.5
PL1TUFF-6	337	16096	0.8	22.0991	13.5	0.0587	13.8	0.0094	2.5	0.18	60.4	1.5	57.9	7.8	-42.1	330.3	60.4	1.5
PL1TUFF-7	277	12297	0.5	21.7293	17.0	0.0611	17.2	0.0096	2.4	0.14	61.8	1.5	60.3	10.1	-1.3	413.2	61.8	1.5
PL1TUFF-8	470	30842	0.6	20.2725	12.3	0.0646	12.4	0.0095	1.6	0.13	60.9	1.0	63.6	7.6	163.4	287.9	60.9	1.0
PL1TUFF-9	484	30018	0.6	21.0206	10.1	0.0632	10.2	0.0096	1.6	0.15	61.8	1.0	62.2	6.1	78.0	239.5	61.8	1.0
PL1TUFF-10	111	3808	0.7	20.8925	40.8	0.0633	41.3	0.0096	6.7	0.16	61.6	4.1	62.3	25.0	92.6	1003.6	61.6	4.1
PL1TUFF-11	438	19502	0.6	21.3066	9.1	0.0625	9.2	0.0097	1.6	0.17	61.9	1.0	61.5	5.5	45.9	217.7	61.9	1.0
PL1TUFF-12	247	10987	0.6	20.1166	19.1	0.0674	19.3	0.0098	2.8	0.15	63.1	1.8	66.2	12.4	181.4	448.9	63.1	1.8
PL1TUFF-13	351	17159	0.7	18.9787	9.4	0.0689	9.6	0.0095	1.9	0.20	60.8	1.1	67.7	6.3	315.5	213.6	60.8	1.1
PL1TUFF-14	161	9660	0.9	23.3520	33.0	0.0559	33.2	0.0095	4.4	0.13	60.8	2.7	55.3	17.9	-177.9	841.5	60.8	2.7
PL1TUFF-15	72	2066	1.1	30.5793	127.1	0.0429	127.4	0.0095	7.7	0.06	61.0	4.7	42.6	53.2	-901.5	0.0	61.0	4.7
PL1TUFF-16	186	12002	0.6	20.9672	19.6	0.0644	19.7	0.0098	2.7	0.14	62.8	1.7	63.4	12.1	84.1	467.8	62.8	1.7
PL1TUFF-17	244	25838	0.8	23.3913	16.3	0.0558	16.4	0.0095	2.4	0.15	60.8	1.5	55.2	8.8	-182.1	408.2	60.8	1.5
PL1TUFF-18	489	35185	0.6	21.6526	9.3	0.0606	9.5	0.0095	1.9	0.20	61.1	1.2	59.8	5.5	7.2	224.6	61.1	1.2
PL1TUFF-19	350	7683	0.9	20.1093	13.0	0.0667	13.1	0.0097	1.8	0.14	62.4	1.1	65.6	8.3	182.3	303.8	62.4	1.1
PL1TUFF-20	104	5165	0.9	28.6039	38.9	0.0455	39.8	0.0094	8.5	0.21	60.6	5.1	45.2	17.6	-711.8	1116.5	60.6	5.1
OR20TUFF-1	372	21537	0.6	19.5608	9.7	0.0680	10.1	0.0096	2.8	0.27	61.9	1.7	66.8	6.5	246.4	223.9	61.9	1.7
OR20TUFF-3	308	12878	0.9	21.6579	13.6	0.0608	13.8	0.0095	2.6	0.19	61.3	1.6	59.9	8.0	6.7	328.0	61.3	1.6
OR20TUFF-6	130	4983	1.3	23.4829	28.7	0.0565	29.1	0.0096	4.6	0.16	61.8	2.8	55.9	15.8	-191.8	731.1	61.8	2.8
OR20TUFF-7	425	18542	0.3	21.2900	14.2	0.0633	14.5	0.0098	3.0	0.21	62.7	1.9	62.3	8.8	47.7	340.2	62.7	1.9
OR20TUFF-8	135	2678	0.7	19.4541	35.6	0.0662	35.9	0.0093	4.7	0.13	60.0	2.8	65.1	22.7	258.9	842.4	60.0	2.8
OR20TUFF-9	193	9491	1.1	21.6720	20.2	0.0599	20.4	0.0094	3.2	0.16	60.4	1.9	59.0	11.7	5.1	490.2	60.4	1.9
OR20TUFF-10	145	5089	0.7	23.4127	41.0	0.0566	41.1	0.0096	3.0	0.07	61.6	1.8	55.9	22.4	-184.4	1063.2	61.6	1.8
OR20TUFF-12	134	16860	1.0	22.0633	24.4	0.0622	24.7	0.0100	3.8	0.15	63.9	2.4	61.3	14.7	-38.2	600.7	63.9	2.4
OR20TUFF-13	137	7752	1.5	26.4461	40.0	0.0487	40.2	0.0093	4.4	0.11	59.9	2.6	48.3	19.0	-498.3	1100.8	59.9	2.6
OR20TUFF-14	234	10401	0.7	21.7367	17.4	0.0630	17.7	0.0099	3.1	0.18	63.7	2.0	62.0	10.6	-2.1	422.8	63.7	2.0
OR20TUFF-15	194	9396	1.0	22.2988	25.8	0.0596	26.0	0.0096	2.9	0.11	61.8	1.8	58.8	14.8	-64.0	638.3	61.8	1.8
OR20TUFF-16	137	4650	1.1	26.8390	76.1	0.0492	76.2	0.0096	3.9	0.05	61.5	2.4	48.8	36.3	-537.7	2403.9	61.5	2.4
OR20TUFF-17	101	6636	1.8	20.2638	63.8	0.0642	64.0	0.0094	5.1	0.08	60.5	3.1	63.1	39.2	164.4	1662.6	60.5	3.1
OR20TUFF-18	630	24145	0.4	21.3511	6.9	0.0634	7.0	0.0098	1.1	0.16	62.9	0.7	62.4	4.3	40.9	166.3	62.9	0.7
OR20TUFF-19	135	8053	1.1	24.3222	33.2	0.0535	33.5	0.0094	4.2	0.12	60.5	2.5	52.9	17.3	-280.5	866.0	60.5	2.5
OR20TUFF-20	544	40037	0.4	22.0967	8.9	0.0598	9.1	0.0096	2.0	0.22	61.5	1.2	58.9	5.2	-41.9	215.4	61.5	1.2
OR21TUFF-1	586	17851	0.6	20.7342	6.7	0.0644	6.8	0.0097	1.5	0.22	62.2	0.9	63.4	4.2	110.5	157.3	62.2	0.9
OR21TUFF-2	185	7096	1.4	20.3639	15.9	0.0650	16.3	0.0096	3.3	0.20	61.5	2.0	63.9	10.1	152.9	374.9	61.5	2.0
OR21TUFF-3	212	8353	0.7	16.4558	33.9	0.0775	34.8	0.0092	7.6	0.22	59.3	4.5	75.8	25.4	631.1	750.8	59.3	4.5
OR21TUFF-4	171	8431	0.7	26.0101	38.8	0.0504	39.0	0.0095	4.0	0.10	61.0	2.4	49.9	19.0	-454.3	1056.3	61.0	2.4
OR21TUFF-5	58	4004	1.7	18.5846	76.0	0.0746	76.5	0.0100	8.8	0.12	64.5	5.6	73.0	53.9	363.0	2054.9	64.5	5.6
OR21TUFF-8	137	4659	0.8	21.0686	24.3	0.0623	24.5	0.0095	2.8	0.11	61.1	1.7	61.4	14.6	72.6	586.2	61.1	1.7
OR21TUFF-9	80	4494	1.4	11.9903	134.0	0.1113	134.2	0.0097	7.1	0.05	62.1	4.4	107.2	137.3	1278.6	329.1	62.1	4.4
OR21TUFF-11	203	950	0.8	18.8202	23.2	0.0711	23.3	0.0097	2.8	0.12	62.3	1.7	69.7	15.7	334.6	531.7	62.3	1.7
OR21TUFF-12	413	17335	0.7	22.0131	11.6	0.0598	11.7	0.0095	1.5	0.13	61.2	0.9	58.9	6.7	-32.6	282.6	61.2	0.9
OR21TUFF-15	102	9270	0.8	16.9593	54.0	0.0774	54.9	0.0095	9.7	0.18	61.1	5.9	75.7	40.0	565.8	1269.8	61.1	5.9
OR21TUFF-16	406	21203	0.7	20.1515	12.8	0.0646	12.9	0.0094	1.6	0.12	60.6	1.0	63.5	7.9	177.4	299.4	60.6	1.0
OR21TUFF-17	185	10398	1.2	21.9373	23.0	0.0593	23.4	0.0094	4.1	0.17	60.5	2.4	58.5	13.3	-24.3	563.4	60.5	2.4
OR21TUFF-18	91	1626	1.2	21.6994	36.2	0.0653	37.1	0.0103	8.0	0.22	65.9	5.3	64.2	23.1	2.1	898.4	65.9	5.3
OR21TUFF-19	121	1865	0.7	18.3515	31.9	0.0726	32.2	0.0097	4.7	0.14	62.0	2.9	71.1	22.1	391.4	732.5	62.0	2.9
OR21TUFF-20	203	360	0.4	15.1032	19.0	0.0903	19.6	0.0099	4.8	0.24	63.5	3.0	87.8	16.5	813.1	399.9	63.5	3.0
OR21TUFF-13	146	1334	0.8	15.4606	29.8	0.0916	30.4	0.0103	5.7	0.19	65.9	3.7	89.0	25.9	763.9	642.4	65.9	3.7
ORtuff-2012-1	175	6779	0.9	18.5031	8.7	0.1292	9.1	0.0173	2.8	0.30	110.8	3.0	123.4	10.6	372.9	196.6	110.8	3.0
ORtuff-2012-2	129	27054	1.7	20.2780	15.3	0.1214	15.3	0.0178	1.3	0.09	114.0	1.5	116.3	16.8	162.8	358.7	114.0	1.5
ORtuff-2012-3	79	9022	0.5	20.5934	17.4	0.1119	17.6	0.0167	2.5	0.14	106.9	2.7	107.7	18.0	126.6	412.3	106.9	2.7
ORtuff-2012-4	96	14449	1.5	23.0490	16.1	0.1098	16.2	0.0183	2.4	0.15	117.2	2.8	105.8	16.3	-145.4	400.4	117.2	2.8
ORtuff-2012-5	113	22590	1.1	21.9631	13.3	0.1112	13.4	0.0177	1.5	0.11	113.2	1.7	107.1	13.6	-27.1	322.7	113.2	1.7
ORtuff-2012-6	189	25543	1.2	19.4839	10.4	0.1332	10.5	0.0188	1.7	0.16	120.2	2.0	127.0	12.5	255.4	238.9	120.2	2.0
ORtuff-2012-7	84	37752	0.9	21.3464	9.8	0.1979	9.9	0.0306	1.7	0.17	194.6	3.2	183.4	16.6	41.4	234.3	194.6	3.2
ORtuff-2012-8	159	18217	1.1	20.9080	5.9	0.1229	6.7	0.0186	3.1	0.47	119.0	3.7	117.7	7.4	90.8	139.4	119.0	3.7
ORtuff-2012-9	445	197927	2.8	20.3440	1.3	0.1604	2.5	0.0237	2.1	0.86	150.7	3.2	151.0	3.5	155.2	29.7	150.7	3.2
ORtuff-2012-10	212	32565	1.4	20.4583	5.8	0.1207	5.9	0.0179	1.3	0.22	114.4	1.5	115.7	6.5	142.1	135.9	114.4	1.5
ORtuff-2012-11	130	10212	1.1	20.2164	8.6	0.1263	8.8	0.0185	1.9	0.21	118.3	2.2	120.8	10.0	169.9	200.4	118.3	2.2
ORtuff-2012-12	423	37157	1.2	20.3430	2.2	0.1270	4.1	0.0187	3.5	0.84	119.6	4.1	121.4	4.7	155.3	51.7	119.6	4.1
ORtuff-2012-13	154	20166	1.5	20.2227	8.2	0.1226	8.4	0.0180	1.6	0.19	114.9	1.8	117.4	9.3	169.2	192.1	114.9	1.8
ORtuff-2012-14	333	20427	0.9	19.1735	10.3	0.1680	10.5	0.0234	1.8	0.18	148.9	2.7	157.7	15.3	292.2	235.9	148.9	2.7
ORtuff-2012-15	400	98331	2.1	20.3312	2.3	0.1582	2.4	0.0233	0.7	0.28	148.7	1.0	149.1	3.3	156.7	54.2	148.7	1.0
ORtuff-2012-16	606	71874	1.9	20.3346	2.1	0.1535	2.4	0.0226	1.1	0.47	144.4	1.6	145.0	3.3	156.3	50.3	144.4	1.6
ORtuff-2012-17	51	4648	0.7	25.4807	52.7	0.0728	52.8	0.0135	3.5	0.07	86.1	3.0	71.3	36.4	-400.4	1464.6	86.1	3.0
ORtuff-2012-18	42	4699	0.7	20.1271	106.3	0.0726	106.7	0.0106	9.1	0.09	67.9	6.1	71.1	73.4	180.2	946.7	67.9	6.1
ORtuff-2012-19	139	47118	2.4	20.8998	7.4	0.1549	7.6	0.0235	1.8	0.24	149.6	2.7	146.2	10.4	91.7	175.7	149.6	2.7
ORtuff-2012-20	225	11331	1.0	20.3388	4.9	0.1250	5.4	0.0184	2.2	0.41	117.8	2.5	119.6	6.0	155.8	114.5	117.8	2.5

Table DR5 - U-Th-Pb TIMS isotopic data for tuff sample PL-1.

	Compositional Parameters						Radiogenic Isotope Ratios									Isotopic Ages					
Sample (a)	Th/U (b)	206Pb* x10-13 mol (c)	mol % 206Pb* (c)	Pb*/Pbc (c)	Pbc (pg) (c)	206Pb/204Pb (d)	208Pb/206Pb (e)	207Pb/206Pb (e)	% err (f)	207Pb/235U (e)	% err (f)	206Pb/238U (e)	% err (f)	corr. coef.	207Pb/206Pb (g)	± (f)	207Pb/235U (g)	± (f)	206Pb/238U (g)	± (f)
z3	0.442	0.2339	94.17%	5	1.20	310	0.141	0.048787	1.216	0.102669	1.301	0.015263	0.110	0.789	138	29	99.24	1.23	97.647	0.107
z8	0.719	0.0359	79.88%	1	0.75	90	0.231	0.050253	7.051	0.068124	7.314	0.009832	0.365	0.732	207	163	66.92	4.74	63.071	0.229
z2	0.548	0.0146	65.31%	1	0.64	52	0.176	0.048390	50.356	0.065357	50.544	0.009796	0.760	0.255	118	1186	64.28	31.48	62.839	0.475
z7	0.737	0.0594	89.12%	3	0.60	166	0.236	0.049731	3.384	0.066365	3.546	0.009679	0.237	0.700	182	79	65.24	2.24	62.092	0.146
z9	0.741	0.0201	86.43%	2	0.26	133	0.238	0.049438	6.181	0.065955	6.355	0.009676	0.281	0.629	169	144	64.85	3.99	62.074	0.174
z1	0.671	0.0348	86.22%	2	0.46	131	0.215	0.046949	5.096	0.062589	5.295	0.009669	0.276	0.733	47	122	61.64	3.17	62.029	0.170
z5	0.632	0.0760	85.95%	2	1.03	128	0.203	0.049473	3.484	0.065947	3.691	0.009668	0.225	0.922	170	81	64.85	2.32	62.023	0.139
z10	0.875	0.0680	89.04%	3	0.69	165	0.280	0.047835	2.838	0.063700	3.003	0.009658	0.187	0.890	91	67	62.70	1.83	61.962	0.115
z12	1.130	0.0665	94.16%	6	0.34	309	0.362	0.048836	1.469	0.065032	1.567	0.009658	0.123	0.811	140	34	63.97	0.97	61.960	0.076
z11	0.646	0.0350	89.40%	3	0.34	170	0.207	0.048947	3.169	0.065176	3.331	0.009657	0.212	0.777	145	74	64.11	2.07	61.957	0.131
z6	0.773	0.0683	91.89%	4	0.50	223	0.248	0.049053	2.020	0.065305	2.146	0.009656	0.151	0.841	150	47	64.23	1.34	61.945	0.093

(a) z1, z2 etc. are labels for fractions composed of single zircon grains or fragments; all fractions annealed and chemically abraded after Mattinson (2005); Zircons labeled with **bold** are included in weighted mean shown in Figure 4

(b) Model Th/U ratio calculated iteratively from radiogenic $^{208}Pb/^{206}Pb$ ratio and $^{206}Pb/^{238}U$ age.

(c) Pb* and Pbc represent radiogenic and common Pb, respectively; mol % ^{206}Pb* with respect to radiogenic, blank and initial common Pb.

(d) Measured ratio corrected for spike and fractionation only. Fractionation estimated at 0.15 +/- 0.03 %/a.m.u. for Daly analyses, based on analysis of NBS-981 and NBS-982.

(e) Corrected for fractionation, spike, and common Pb; all common Pb was assigned procedural blank: $^{206}Pb/^{204}Pb = 18.042 \pm 0.61\%$; $^{207}Pb/^{204}Pb = 15.537 \pm 0.52\%$; $^{208}Pb/^{204}Pb = 37.686 \pm 0.63\%$ (all uncertainties 1-sigma).

(f) Errors are 2-sigma, propagated using the algorithms of Schmitz and Schoene (2007).

(g) Calculations are based on the decay constants of Jaffey et al. (1971). $^{206}Pb/^{238}U$ and $^{207}Pb/^{206}Pb$ ages corrected for initial disequilibrium in $^{230}Th/^{238}U$ using Th/U [magma] = 3.